ANL-6336
Reactor Technology
(TID-4500, 16th Ed.,
Amended)
AEC Research and
Development Report

ARGONNE NATIONAL LABORATORY
9700 South Cass Avenue
Argonne, Illinois

CRITICAL STUDIES OF A 450-LITER URANIUM OXIDE FAST REACTOR CORE (ZPR-III Assembly 29)

by

A. L. Hess, W. Gemmell,*
J. K. Long, and R. L. McVean

Idaho Division

Work Completed November 1960

*Attached to ANL from UKAEA,
DERE, Thurso, Caithness, Scotland

Operated by The University of Chicago
under
Contract W-31-109-eng-38

DISCLAIMER

TABLE OF CONTENTS

LIST OF FIGURES

LIST OF TABLES

LIST OF TABLES

CRITICAL STUDIES OF A 450-LITER URANIUM OXIDE FAST REACTOR CORE (ZPR-III Assembly 29)

by

A. L. Hess, W. Gemmell,
J. K. Long, and R. L. McVean

ABSTRACT

Results of studies with ZPR-III Assembly 29, a mockup of a typical, dilute UO_2-fueled fast reactor, are reported. The assembly consisted of a 454-liter cylindrical core, blanketed with depleted uranium, with a critical mass of 421 kg U^{235}. Experiments included measurements of fission rates, material reactivity worths, and Rossi alpha. The results of multigroup calculations using the present Argonne cross-section sets are presented, and discrepancies between experimental results and calculations are discussed.

INTRODUCTION

It is anticipated that the use of oxides and carbides of uranium and plutonium in reactor fuel elements will overcome the low fuel-burnup limitations present with metallic fuels. It has been found that UO_2 can sustain economic burnups (>5 a/o) without showing evidence of radiation damage.

Some preliminary design studies of oxide-fueled fast reactor systems have been published, based on current cross-section data. The earliest study was conducted in 1957[1] with a mixed PuO_2-UO_2 fuel, and this work has lately been extended.[2] The reactor considered would use 500 kg or more of plutonium to operate at 1000 ± 200 Mw. Physics calculations for large uranium and plutonium oxide reactors have been made by Okrent and Loewenstein,[3] and recently data on 800- to 1500-Mw oxide reactors have been given by Okrent.[4] However, no experimental data have been available to supplement the parametric surveys. To provide such data and to evaluate the theoretical designs, a series of studies was begun in September 1960 with the ZPR-III critical facility to determine the properties of uranium-oxide and -carbide compositions.

The first of these studies, known as Assembly 29, was a mockup of a dilute, UO_2-fueled fast reactor. This paper presents a description of the assembly and the experiments performed with it. Included are comparisons of measurements with SNG predictions and criticisms of the multigroup sets used.

I. DESCRIPTION OF ASSEMBLY

A. Preliminary Design: Initial Composition

The assembly was to represent a hypothetical UO_2-fueled power reactor: a large cylindrical core, with a composition of about 25 v/o UO_2, 25 v/o steel, and 50 v/o coolant (Na), blanketed with depleted uranium. The size of the assembly built was limited only by the material available. In view of this, and for convenience of construction, the composition chosen was 30 v/o UO_2, with the uranium 31% enriched.

The ZPR machine, shown in Fig. 1, consists of one fixed and one movable half, each an array of square matrix tubes into which are inserted drawers containing the materials to be used in the reactor.

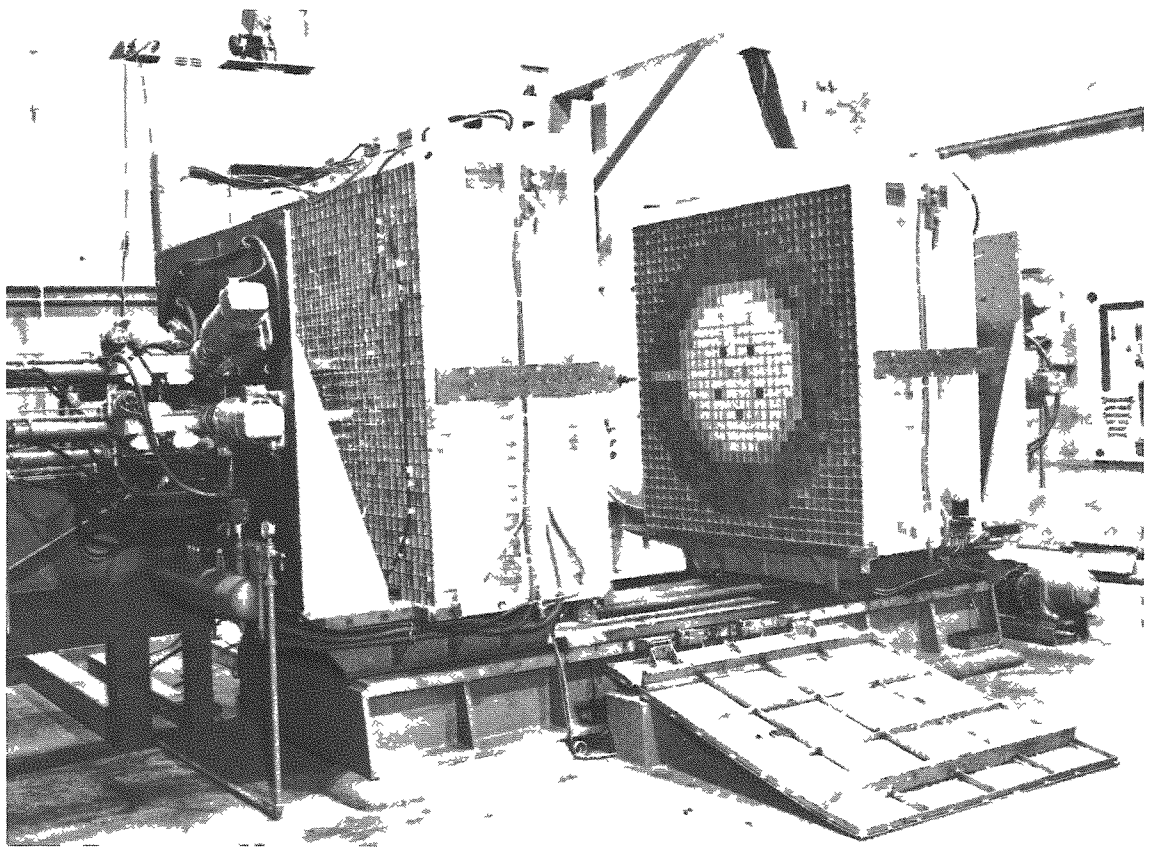

Fig. 1. Zero Power Reactor No. III (ZPR-III) Critical Facility

Typically loaded drawers are shown in Fig. 2. (A complete description of the ZPR facility and methods of assembly construction has been given by Cerutti et al.[5]

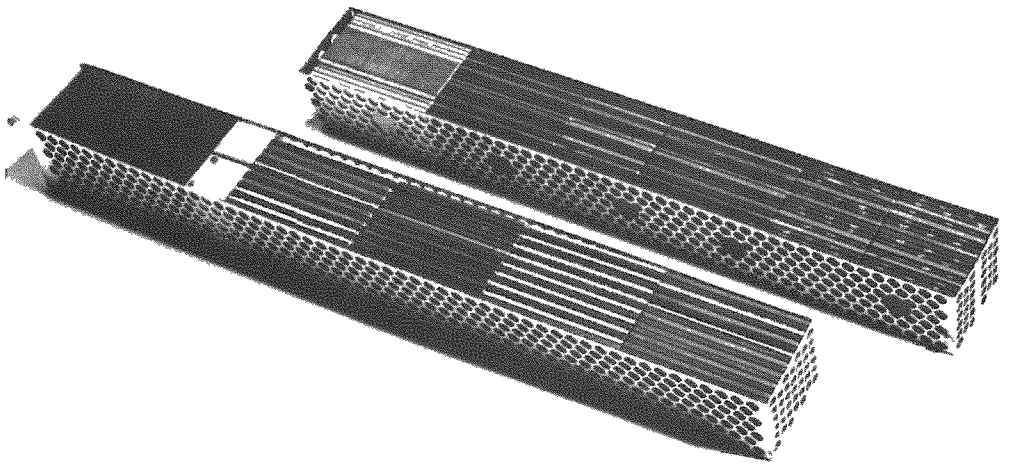

Fig. 2. Typical Assembly Drawers

Construction of this assembly involved various approximations. Uranium oxide, which was unavailable, was simulated by having plates of sintered aluminum oxide adjacent to uranium plates. Two alumina plates per plate of uranium gave an atomic ratio for uranium to oxygen of 1:1.90. Also, the sodium coolant was mocked with aluminum to simulate the characteristics of sodium. Previous fast critical studies had shown that 48 v/o Na could be represented by about 25 v/o Al.

It was planned to construct the core entirely of drawers loaded as shown in Fig. 3, with a resulting composition, including steel of the drawers and matrix tubes, as given in Table I. Using this composition, an S4 calculation predicted a critical volume of 380 liters, and for the geometry intended (L/D = 0.9) the core length was set at 28 in. The arrangement of material in the drawers approximated that in a power reactor: the fuel, UO_2, is clad in stainless steel and surrounded by coolant. The blanket thickness was chosen as 12 in. radially and axially.

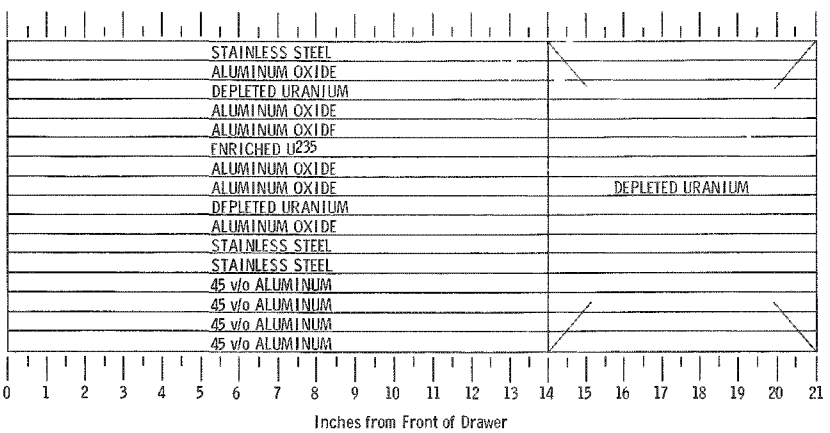

Fig. 3. Standard Core Drawer - Top View

Table I

INITIALLY PLANNED CORE COMPOSITION

Material	Number of $\frac{1}{8}$-in. Columns per Drawer
93% Enriched Uranium	1
Depleted Uranium	2
Stainless Steel	3
45 v/o Al (perforated)	4
Al_2O_3	6

Material	Density (gm/cc)	Volume Percent
U^{235}	0.873	4.66
U^{238}	1.957	10.30
Steel	1.937	24.67
Al	0.658	24.38
O	0.370	14.52

It is estimated that about 10% of all fissions in the core occur in U^{238}. Using the delayed-neutron data given by Keepin,(6) the following parameters were adopted throughout the study for converting measured periods to reactivity values:

$\beta_{eff} = 0.0073$ $\qquad$ \$1.00 = 327 inhours

$\ell \approx 8 \times 10^{-8}$ sec $\qquad$ 1 inhour = $2.23 \times 10^{-5} \Delta k/k$.

The period-to-inhour conversion curve used is shown in Fig. 4.

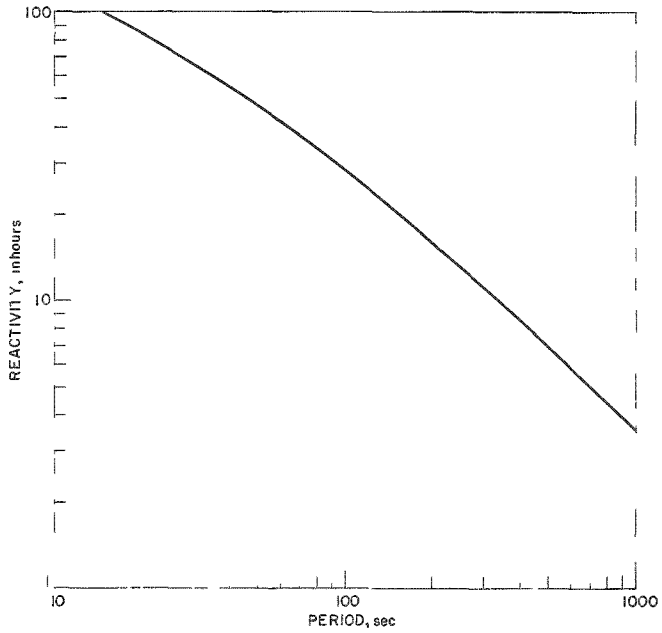

Fig. 4

Inhour Curve

B. Approach to Critical: Increasing Enrichment

After loading the blanket outline, the approach to critical was begun by stepwise radial additions of core drawers of the type shown in Fig. 3. The loading surpassed the 332-kg estimate, and drawer addition was discontinued when the loading reached 396.6 kg U^{235}. At this point, the assembly was still subcritical and the supply of Al_2O_3 was used up.

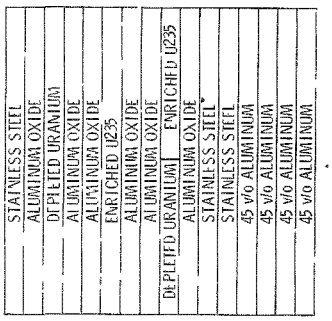

Fig. 5. "Seeded" Core Drawer - Front View

It was then decided to approach criticality by increasing the uranium enrichment. This was accomplished by substitution of enriched uranium for depleted uranium in $\frac{1}{2}$ column per drawer of a uniform distribution of drawers. A front view of this type of drawer with $1\frac{1}{2}$ columns enriched uranium is shown in Fig. 5. The number of drawers thus "seeded" was increased in steps. Criticality was obtained when 56 of the 416 core drawers were seeded. The U^{235} loading was 422.9 kg.

The approach to critical above 300 kg is shown in Fig. 6, where the inverse count rate of BF_3 counters is plotted versus the U^{235} loading. Extrapolation from the curve below 400 kg indicates that the critical mass with the initial composition (Table I) would be in excess of 450 kg.

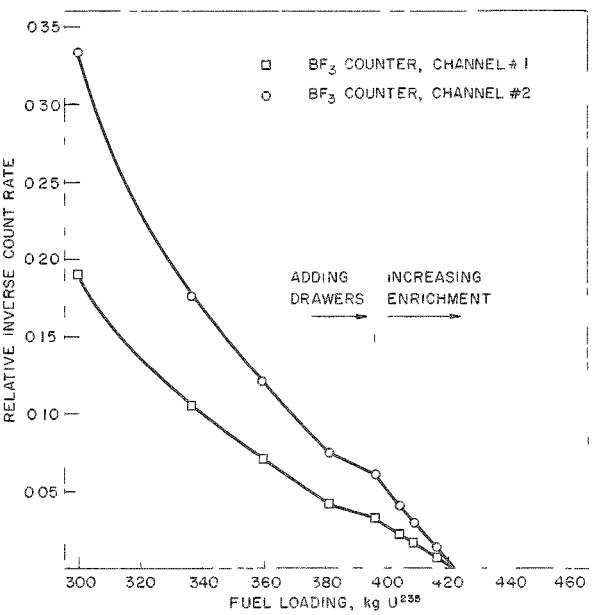

Fig. 6
Approach to Critical

C. Dimensions of Assembly

Figures 7 and 8 are midplane diagrams of halves 1 and 2 of the assembly at the critical loading, and Fig. 9 shows the axial geometry.

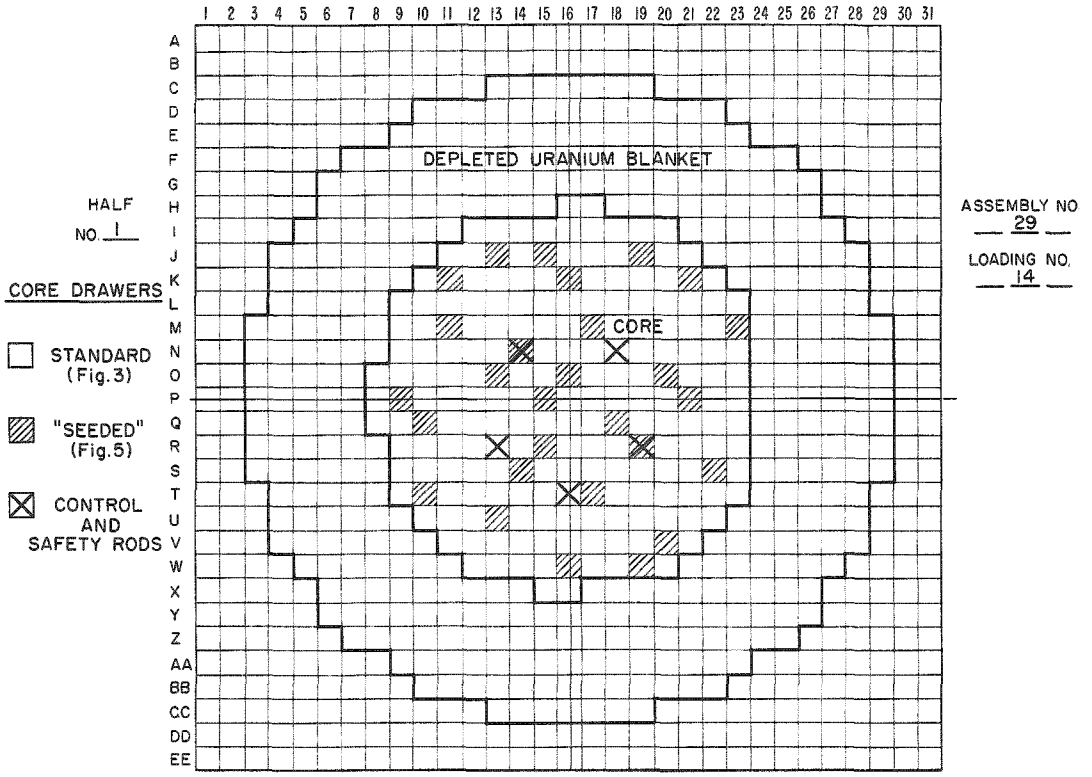

Fig. 7. Interface View of Assembly - Half #1

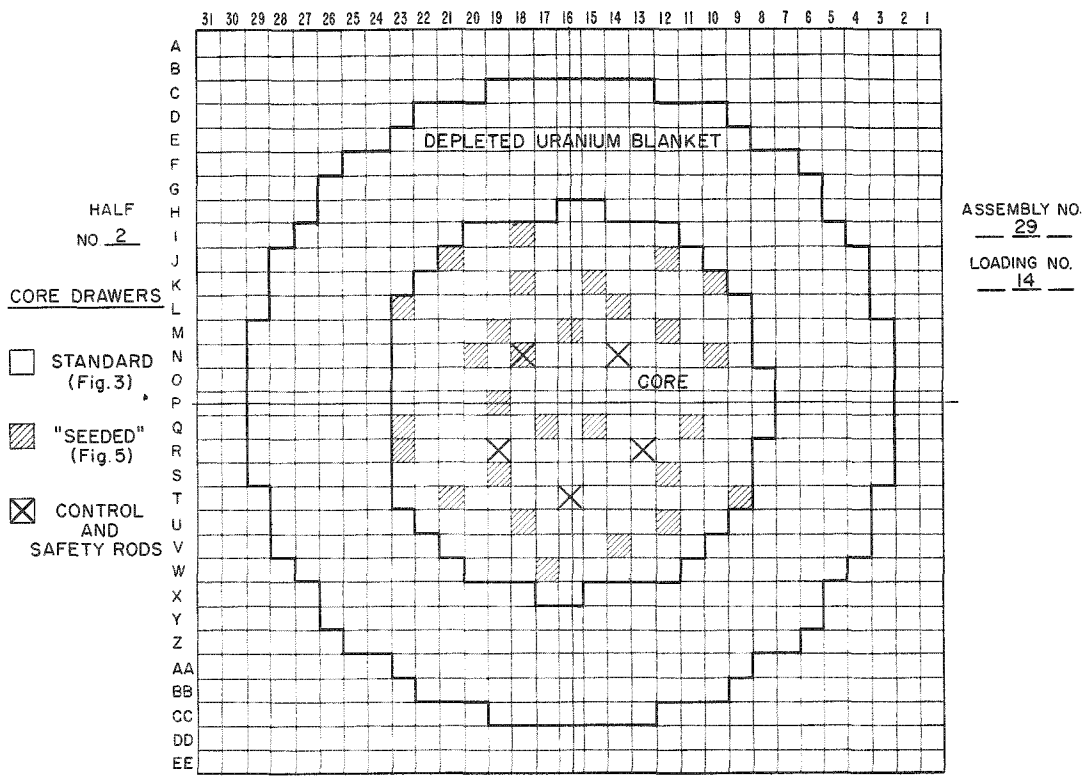

Fig. 8. Interface View of Assembly - Half #2

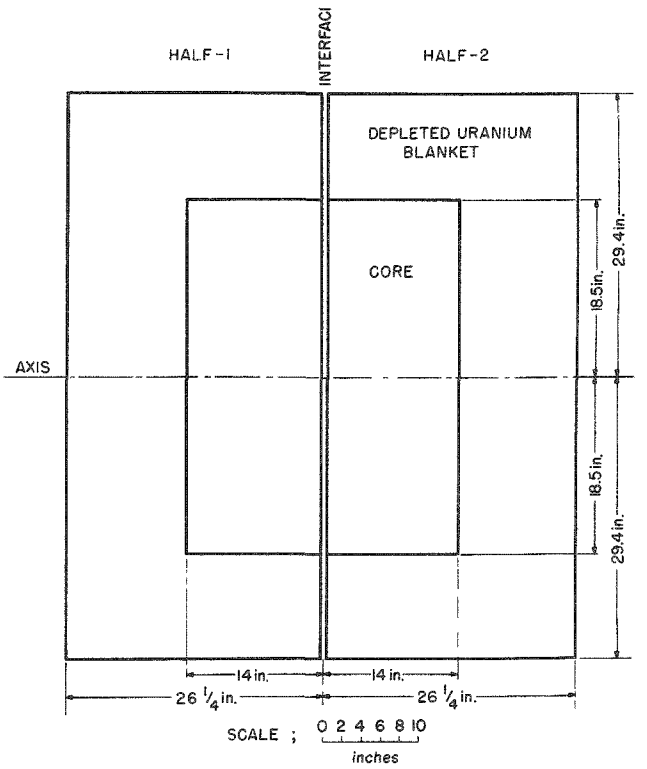

Fig. 9

Vertical Section through Assembly Axis

Dimensions are given in Table II; these were calculated with the aid of the ZPR-III specifications given in Appendix A.

Table II

DIMENSIONS OF ASSEMBLY 29

Core:		
	Length	28.06 in. (71.27 cm)
	Diameter (average)	35.48 in. (90.12 cm)
	L/D	0.792
	Volume	454.3 liters
Blanket:		
	Axial Thickness	12.0 in. (30.48 cm)
	Radial Thickness (average)	11.8 in. (29.97 cm)

D. Composition of Critical Loading

The average composition of the assembly, as shown in Figs. 7, 8, and 9, is given in Table III.

Table III

FINAL COMPOSITION OF ASSEMBLY 29

	Core Composition		Blanket Composition	
Material	gm/cc	v/o	gm/cc	v/o
U^{235}	0.931	4.97	0.036	0.19
U^{238}	1.896	9.98	15.8	83.3
Steel	1.932	24.6	0.574	7.31
Al	0.658	24.4		
O	0.370	14.5		

E. Critical Mass: Fuel Worth at Core Edge

The 422.9-kg loading of the assembly was 42.8 ± 0.4 inhours supercritical with all rods in. The worth of two standard drawers relative to the blanket at the core edge was found to be 37.7 ± 0.4 inhours. Also, a substitution of depleted uranium for enriched uranium in two standard drawers at the core edge gave a (34.4 ± 0.4)-inhour loss. From these data, an average worth of 19.65 ± 0.21 inhours/kg U^{235} is derived for average core material at the core edge.

The clean critical mass then calculated is 420.73 ± 0.04 kg U^{235}; the critical volume is 452 liters. Also, for the relation $\Delta k/k = (1/f)\Delta M/M$ (fuel addition) at the core edge, a value of f = 5.42 is obtained. This compares favorably to a value of 5.2 calculated by means of a one-group theory approximation.

II. MULTIGROUP CRITICALITY CALCULATIONS

A. SNG Prediction of Critical Mass with Initial Composition

Prior to the construction of the assembly, an SNG-S_4 problem was run, using the 11-group cross-section Set 58,[7] to predict the critical size. The calculation determined the critical volume of a homogeneous spherical core, blanketed by 12 in. of depleted uranium, with the composition indicated in Table IV. This table corresponds to the initially planned composition (see Table I) except for slight differences in U^{235}, Al, and O core-volume fractions, and a stainless steel value that is +9% in error.

Table IV

SNG COMPOSITION INPUT

Material	Core (v/o)	Blanket (v/o)
U^{235}	4.68	0.19
U^{238}	10.31	83.3
Stainless Steel	26.93	7.31
Al	24.10	
O	14.29	

The critical volume for the sphere given by the calculation was 387 liters, equivalent to a critical mass of 339 kg. For the actual assembly a -5% adjustment is used to account for heterogeneity,[8] and for the proposed cylinder (L/D = 0.9) a +3% shape factor is needed.[9] The predicted critical mass for the initial composition was then 332 kg, and the critical volume 379 liters.

The actual critical mass that would have been obtained with the initial composition can be roughly determined from the approach curves. The subcriticality of the loading where fuel enrichment was begun (397 kg) can be estimated from the curves after 397 kg. Then, using the relationship $\Delta k/k = (1/f)\Delta M/M$ for fuel addition at the core edge, and the experimental "f-value" of 5.4, the true critical mass would be about 460 kg U^{235}.

The SNG prediction of 332 kg is thus low by 28%, equivalent to about 5.2% Δk. This discrepancy indicates inaccuracies in the cross-section set used. Adjustments to this set are being sought.

B. SNG k Calculations for Final Assembly

Based on the final composition of the assembly and its critical volume, a few SNG-S_4 k calculations were performed using three different cross-section sets[7,10,11] to observe whether or not superior prediction of the critical mass of the assembly could have been possible. The problem inputs prescribed a homogeneous spherical core of 47.7-cm radius, with a composition given in Table III, blanketed by about 12 in. of depleted uranium. The reactivity eigenvalues calculated are presented in Table V. All the calculations used the same number of mesh points except the last (denoted by the asterisk), in which the number of mesh points was increased by a factor of four to see what effect the change might have.

Again, errors in the cross-section sets are indicated by the results. For previous dilute assemblies, multigroup theory has provided critical masses which compare to experimental values to within ±2.5% Δk.

Table V

REACTIVITY FACTOR k FOR FINAL ASSEMBLY

	Multigroup Theory			
Experimental	11-group Set #58	10-group Set #89	16-group Set #135	16-group* Set #135
1.000	1.058	1.045	1.051	1.050

III. CONTROL ROD CALIBRATION

Drawers used for reactor control rods were of the "seeded" type, with $1\frac{1}{2}$ columns of enriched uranium. Control Rod No. 1 was in drawer 2N-18 and Rod No. 10 was in 1-N-14. Rod No. 10 was calibrated for reactivity measurements by observing periods corresponding to changes in rod position. These periods were then translated into reactivity in inhours using the conversion curve given in Fig. 4. The calibration is presented in Table VI and graphed in Fig. 10.

Table VI

CONTROL ROD CALIBRATION

Rod No. 10 Position From Full Insertion (in.)	Reactivity	
	Inhours	$\Delta k/k \times 10^5$
0.000	0.00	0
1.000	7.07	15.77
2.000	14.84	33.09
4.000	32.27	71.96
6.000	49.77	110.99
7.668	63.72	142.10
9.690	79.8	177.95

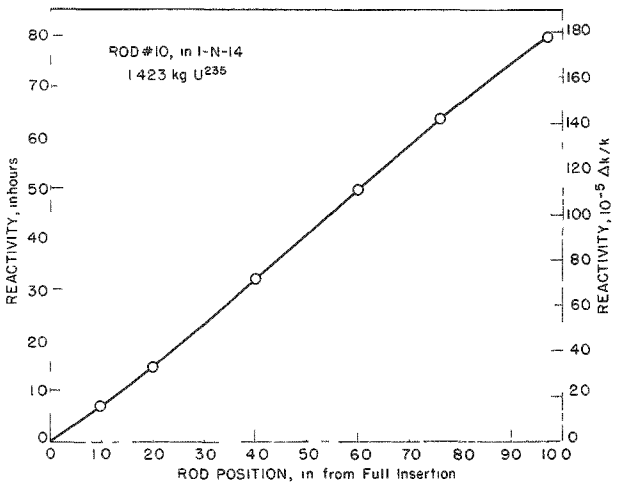

Fig. 10

Control Rod Calibration

IV. MEASUREMENT OF ROSSI ALPHA

Rossi alpha, $\alpha = -\beta_{eff}/\ell$, was determined for this assembly at delayed critical using the method described by Brunson et al.[12] From the values of α measured at 15 subcritical points, the extrapolated delayed critical value was $\alpha = (-3.17 \pm 0.10) \times 10^4$. Assuming $\beta_{eff} = 0.0073$, the neutron lifetime was then $(23.0 \pm 0.7) \times 10^{-8}$ sec.

V. REACTIVITY WORTHS OF MATERIALS

For the experiments measuring changes in reactivity due to material substitutions, the following procedure was used: the position of Control Rod No. 10 at criticality was determined both before and after the substitution; during each run the determination of the critical rod position was augmented by a period measurement with the rod inserted a few inches from the critical position. The substitution worths were found from the rod calibration and considered to be accurate to ± 0.4 inhour or $10^{-5}\Delta k$, a limit set by the reproducibility in closure of the machine halves.

A. Worth of Blanket Material at Core Edge

A substitution of void for depleted uranium was made in the first inch of axial blanket (14 to 15 in. in Figs. 3 and 5) of the central nine drawers in each half. A total of 10.112 kg of depleted uranium was removed; the resulting loss of reactivity was 9.98 inhours, indicating a worth of 0.987 ± 0.04 inhour/kg. Taking the U^{235} content (using data in Table XV later) into consideration, a reactivity coefficient of 0.921 ± 0.04 inhour/kg U^{238} or $0.489 \pm 0.02 \times 10^{-5}$ Δk/mole U^{238} was obtained.

B. Distributed Worths of Al and O

The average worths of aluminum and oxygen throughout the core were determined from reactivity changes resulting from slight changes in the average aluminum and oxygen compositions of the core. Substitutions were made of 45 v/o Al for Al_2O_3, and then 100 v/o Al for 45 v/o Al, in one column per drawer of 10 drawers distributed evenly in one-half of the assembly. The drawers of the distribution (shown in Fig. 11) have a rms distance from the core axis of 12.74 in. compared to 12.53 in. for all of the core drawers. The results of the substitution thus should provide average worths over the whole core. The experimental results were:

Substitution	Worth
-1.432 kg Al_2O_3 +6.59 kg Al	-9.20 ± 0.4 inhours
+0.8272 kg Al	$+3.45 \pm 0.4$ inhours

From these data were derived the distributed worths given in Table VII.

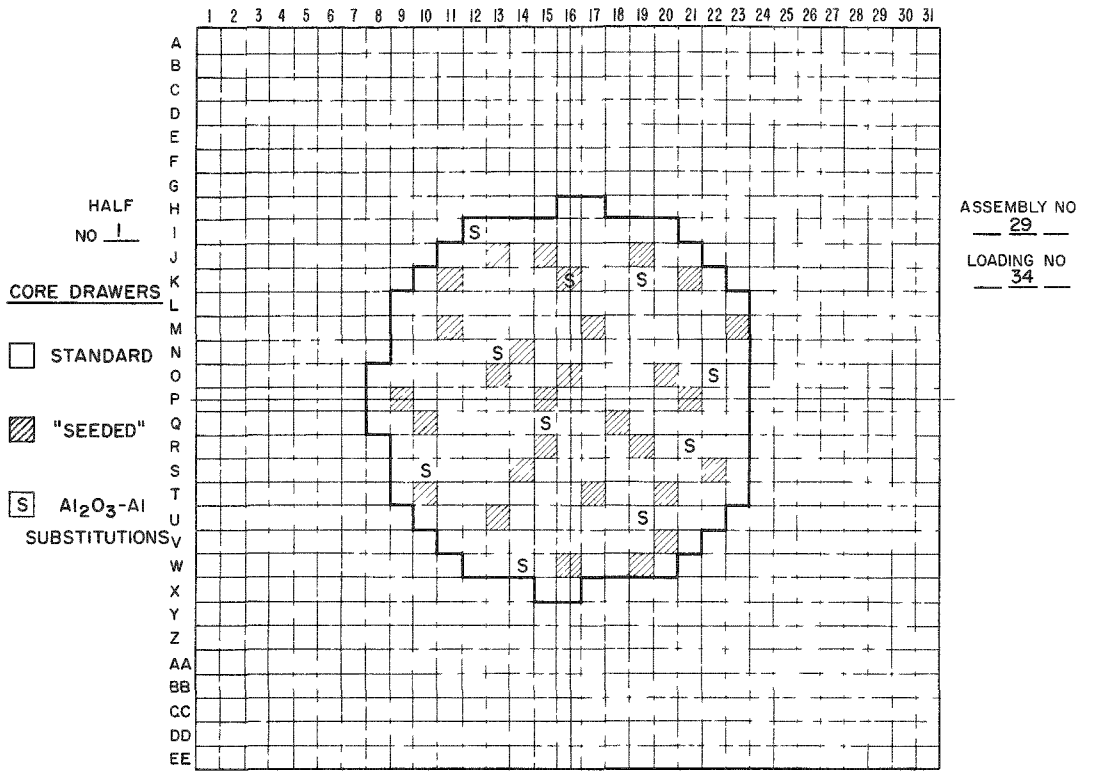

Fig. 11. Distribution of Drawers for Al_2O_3-Al Substitutions

Table VII

DISTRIBUTED REACTIVITY WORTHS

Material	Worth	
	Inhours/kg	Δk/mole x 10^5
Al	4.17 ± 0.49	0.251 ± 0.029
Al_2O_3	8.34 ± 0.32	1.897 ± 0.073
O	13.05 ± 0.57	0.466 ± 0.020

C. Central Reactivity Coefficients

Reactivity worths of various elements were measured at the core center. Samples of fissile and nonfissile materials were substituted for void in the front end of the two central drawers (1- and 2-P16 of Figs. 7 and 8). The effect on the material worths of making the fuel more homogeneous in the central core region was also determined.

1. Fissile materials, 2 x 2 x $\frac{1}{4}$-in. samples: The reference loading for the small fissile samples had 45% aluminum and 63% aluminum in the first $\frac{1}{4}$ in. of the central drawers 1- and 2-P-16. The fissile materials were substituted either clad in or sandwiched between 100% aluminum such that the net aluminum change was negligible. In Table VIII the experimental results are presented, along with the isotopic reactivity coefficients derived from the data.

Table VIII

CENTRAL WORTHS OF FISSILE MATERIALS

Material	Sample Mass, (kg)	Worth of Sample, (inhours)	Material Worth, (inhours/kg)	Isotope Worth $\Delta k/mole \times 10^5$
Depleted Uranium	0.2965	-2.15	-7.25	U^{238} -3.89 ± 0.72
93% Enriched Uranium	0.2878	+34.9	+121.2	U^{235} 68.4 ± 0.8
Pu (95% Pu^{239}, 5% Pu^{240})	0.1860	+38.6	+207.5	Pu^{239} 116.5 ± 0.8
U^{233} (2.4% U^{238})	0.2265	+54.1	+238.9	U^{233} 127.2 ± 0.9

2. Nonfissile materials, 8-cu-in. samples, normal core: For the less reactive materials, larger samples were needed to attain reasonable accuracy. An 8-cu-in. void was created at the core center by recessing the core material one inch in the center drawer of each half of the assembly. Samples, 2 x 2 x 1 in., were substituted in these spaces and the reactivity change was measured. The experimental results are given in Table IX.

Table IX

CENTRAL WORTHS OF U^{238}, Al, C, AND Fe; NORMAL CORE

Material	Sample Mass, (kg)	Worth of Sample,* (inhours)	Material Worth	
			Inhours/kg	$\Delta k/mole \times 10^5$
Aluminum	0.3508	+1.05	2.99 ± 1.1	0.18 ± 0.07
Depleted Uranium	2.460	-15.55	-6.32 ± 0.16	(U^{238}) -3.50 ± 0.09
Graphite	0.1964	+7.75	+39.5 ± 2.0	1.06 ± 0.05
Stainless Steel	1.017	-1.35	-1.33 ± 0.40	(Fe) -0.16 ± 0.05**

*Accurate to ± 0.4

**Considering Cr and Ni like Fe

3. Nonfissile materials, 8-cu-in. samples. Effects of fuel heterogeneity: An effort was made to determine the effects of fuel heterogeneity on the neutron spectrum and material worths. The fuel in the central region of the core was made more homogeneous by splitting the $\frac{1}{8}$ -in. enriched uranium columns into two separate $\frac{1}{16}$ -in. columns in the nine central

drawers of each half. The "unbunched" drawer arrangements are shown in Figs. 12 and 13. With the core thus "unbunched," the worths of the samples listed in Table IX were remeasured. The results, however, were inconclusive. Table X presents the experimental data.

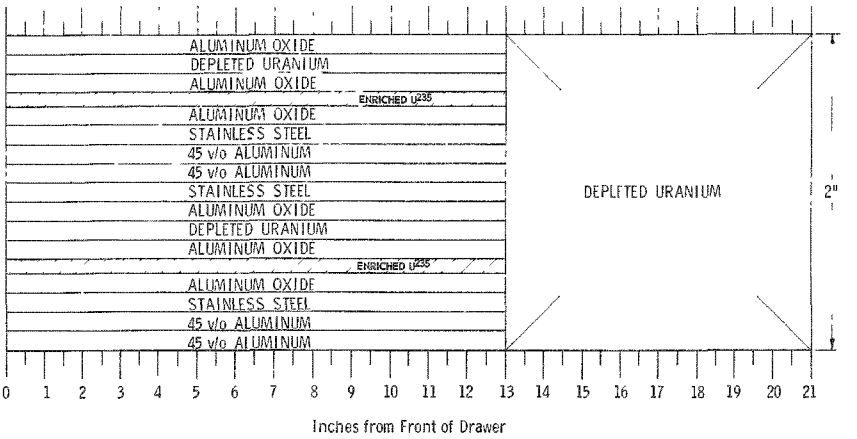

Fig. 12. Standard Core Drawer with Fuel "Unbunched" - Top View

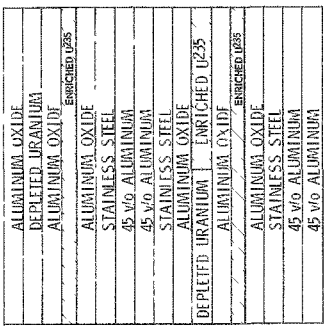

Fig. 13.

Seeded Core Drawer with Fuel "Unbunched" - Front View

Table X

CENTRAL WORTHS OF U^{238}, Al, C AND Fe; FUEL "UNBUNCHED" IN CENTRAL CORE REGION

Material	Sample Mass, (kg)	Worth of Sample, [inhours (accuracy of ±0.4)]	Material Worth	
			Inhours kg	Δk, mole x 10^5
Aluminum	0.3508	+0.45	+1.28 ± 1.1	0.077 ± 0.068
Depleted Uranium	2.400	-16.10	-6.52 ± 0.16	(U^{238}) -3.61 ± 0.09
Graphite	0.1964	+8.20	+41.6 ± 2.0	1.11 ± 0.05
Stainless Steel	1.017	-1.90	-1.87 ± 0.40	(Fe) -0.23 ± 0.05

It can be seen that the values in Table X differ slightly from those in Table IX. However, the deviations could be attributed to experimental error, and it cannot be concluded with certainty that the heterogeneity change affected the material worths. Included in Tables IX and X are the reactivity coefficients in Δk/mole for the major constituents of the materials measured. The values for iron are approximations; it was assumed that the Cr and Ni in the steel have the same worth as Fe.

Substitution of samples at the center was continued with the "unbunched" core, measuring the worths of numerous materials associated with fast reactors. The results are tabulated in Table XI. Some of these samples were clad in stainless steel, but the sample worths listed have been corrected for the steel effects.

Table XI

CENTRAL WORTHS OF NONFISSILE MATERIALS; FUEL "UNBUNCHED" IN CENTRAL CORE REGION

Material	Sample Mass, (kg)	Worth of Sample, [inhours (accuracy of ±0.4)]	Material Worth	
			Inhours/kg	Δk/mole x 10^5
Ag	0.6831	-38.15	-55.8 ± 0.5	-13.43 ± 0.14
Al_2O_3	0.3237	+4.40	+13.6 ± 1.2	(O) 0.97 ± 0.10
B (92 a, o B^{10})	0.024	-54.8	-2284 ± 17	(B^{10}) -59.4 ± 0.4
B_4C (90 a o B^{10})	0.0321	-52.6	-1640 ± 12	(B^{10}) -59.2 ± 0.4
Ba	0.3324	+2.81	+8.70 ± 1.24	2.67 ± 0.38
Be	0.1204	+12.85 ± 2	+106.8 ± 16	2.15 ± 0.34
Bi	1.276	+0.80	+0.63 ± 0.32	0.29 ± 0.15
CH_2	0.0146	+17.70	+1214 ± 27	(H) 18.42 ± 0.42
Core Material	0.7783	+15.12	+19.5 ± 0.5	
Hf	1.654	-33.58	-20.27 ± 0.24	-8.08 ± 0.10
Hg	1.383	-7.73	-5.58 ± 0.29	-1.02 ± 0.05
Mo	1.280	-15.05	-11.78 ± 0.31	-2.52 ± 0.06
Na	0.091	+1.61	+17.7 ± 4.4	0.91 ± 0.23
Nb	0.4896	-9.36	-19.15 ± 0.82	-3.97 ± 0.17
Pb	1.475	-0.25	-0.17 ± 0.27	-0.078 ± 0.13
Physicum I*	0.232	-4.64	-20.0 ± 1.7	
Physicum II*	0.210	-3.14	-15.0 ± 1.9	
Ru	0.228	-7.22	-31.8 ± 1.8	-7.21 ± 0.40
S	0.1998	-2.03	-10.2 ± 2.0	-0.73 ± 0.15
Sn	0.9477	-6.38	-6.73 ± 0.42	-1.78 ± 0.11
Ta	0.507	-16.50	-32.5 ± 0.8	-13.11 ± 0.32
Th	1.488	-22.25	-14.95 ± 0.27	-7.75 ± 0.14
V	0.5272	+2.75	+5.21 ± 0.76	0.59 ± 0.08
Y	0.5821	0.45	+0.77 ± 0.67	0.15 ± 0.14
Zr	0.846	-1.35	-1.60 ± 0.47	-1.46 ± 0.43

* Mixture of typical fission product elements (Reference 13).

The material worths are expressed as Ih/kg of the sample material and also as the Δk/mole derived for the principal element or isotope contained in the material. In deriving the B^{10} worth from the enriched B and

enriched B_4C worths, it was assumed that only B^{10} and C contributed reactivity effects. The makeup of these materials is as follows:

Enriched B = 94 w/o B, 6% impurities;
B = 92 a/o B^{10}

Enriched B_4C = 69.3 w/o B, 30.7% C;
B = 90.7 a/o B^{10}

D. Reactivity Coefficient Axial Traverses

The reactivity worths of U^{235}, U^{238}, Pu^{239}, and B^{10} as a function of axial position were determined by traversing small samples of these materials along the core axis. The center drawers were modified to allow insertion of a guide tube through which the samples were moved remotely. Control rod positions at criticality were recorded for the various axial positions of the sample. Traverses also were made of the drive rod without a sample and with a blank representing the Pu^{239} and B^{10} canning material. Sample specifications are given in Table XII, and Table XIII presents the experimental data. The critical rod positions are considered to be accurate to ±0.010 in. or about ±0.08 inhour; closure of the halves is not involved in these measurements.

Table XII

SPECIFICATIONS OF TRAVERSE REACTIVITY SAMPLES

Reactive Material	Mass, (g)	Composition	Length, (in.)	Diameter, (in.)
Enriched Uranium	22.93	93.1% U^{235}, 6.9% U^{238}	$\frac{1}{2}$	$\frac{7}{16}$
Natural Uranium	64.39	99.3% U^{238}, 0.7% U^{235}	2	$\frac{3}{8}$
Plutonium*	24.09	94.9% Pu^{239}, 0.3% Pu^{241}, 4.8% Pu^{240}	$\frac{1}{2}$	$\frac{1}{2}$
Enriched B*	3.25	97.5% B, B = 84.6 a/o B^{10}	2	$\frac{1}{2}$

*In stainless steel can

Table XIII

AXIAL TRAVERSES OF REACTIVITY SAMPLES

Sample Distance from Core Center (in.)	Rod No. 10 Position at Criticality (in. from full insertion)					
	No Sample	Enriched Uranium	Natural Uranium	Blank	Plutonium	Enriched Boron
Reference	5.610	5.565	5.655	5.644	5.630	5.630
-26	5.590*	5.585	5.685			
-21				5.643	5.632	5.615
-20	5.594*	5.598	5.685			
-14	5.610	5.688	5.700	5.678	5.821	5.440
-12	5.630	5.745	5.690			
-10	5.640	5.805	5.685			
-8	5.655	5.853	5.685			
-7				5.700	6.099	4.945
-6	5.670	5.890	5.690			
-4	5.675	5.930	5.700			
-2	5.675	5.945	5.685			
0	5.670	5.940	5.685	5.705	6.240	4.710
2	5.665	5.935	5.695			
4	5.663	5.925	5.695			
6	5.670	5.895	5.695			
7				5.705	6.125	4.945
8	5.672	5.857	5.715			
10	5.672	5.835	5.725			
14				5.749	5.895	5.500
20.45				5.750	5.750	5.720

*Questionable values.

In Table XIV are listed the reactivity coefficients of U^{235}, U^{238}, Pu^{239}, and B^{10} corresponding to axial position as derived from the data in Table XIII. In obtaining the worths of Pu^{239}, it was assumed that the reactivity of the sample was due only to the Pu^{239} and Pu^{241} present, that the effect of Pu^{240} would not be discernible, and that Pu^{241} was worth as much as Pu^{239}. Also, the worth of the boron sample was taken as that of the B^{10} present. The values in Table XIV are plotted in Figs. 14 and 15.

Table XIV

AXIAL REACTIVITY COEFFICIENTS

Distance from Interface (in.)	Isotope Worth, (Δk/mole x 10^5) U^{235} ($\pm$3.0)*	U^{238} ($\pm$1.0)*	Pu^{239} ($\pm$2.9)*	B^{10} ($\pm$1.0)*
-26	8.6**	3.6**		
-21			0.2	-1.03
-20	10.4	3.2		
-14	26.3	3.1	31.8	-16.6
-12	34.2	0.8		
-10	44.9	-0.3		
-8	51.9	-1.5		
-7			83.6	-54.7
-6	56.6	-2.2		
-4	64.1	-1.9		
-2	67.3	-3.0		
0	67.3	-2.7	111.2	-77.0
2	67.3	-1.6		
4	65.6	-1.4		
6	58.2	-1.8		
7			87.9	-55.1
8	49.1	-0.5		
10	44.5	+0.5		
14			32.4	-19.8
20.45			2.8	-1.2

*Accuracy

**Doubtful values.

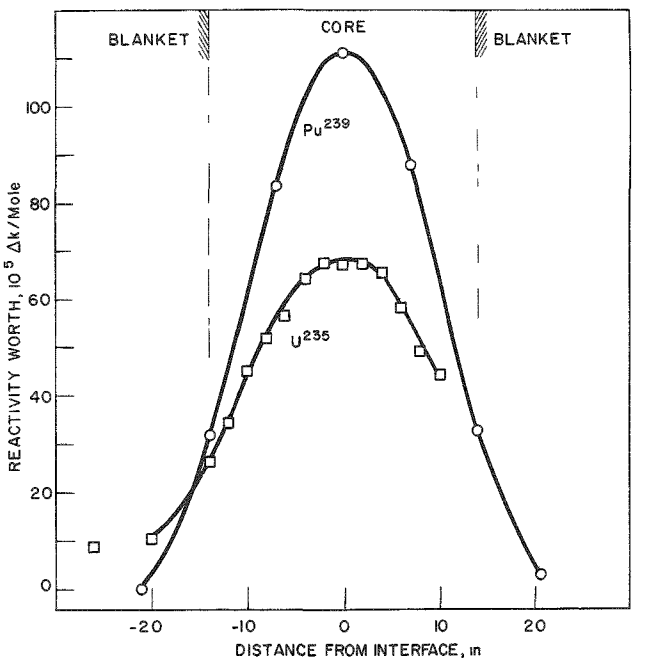

Fig. 14

Pu^{239} and U^{235} Reactivity Coefficients Along Axis

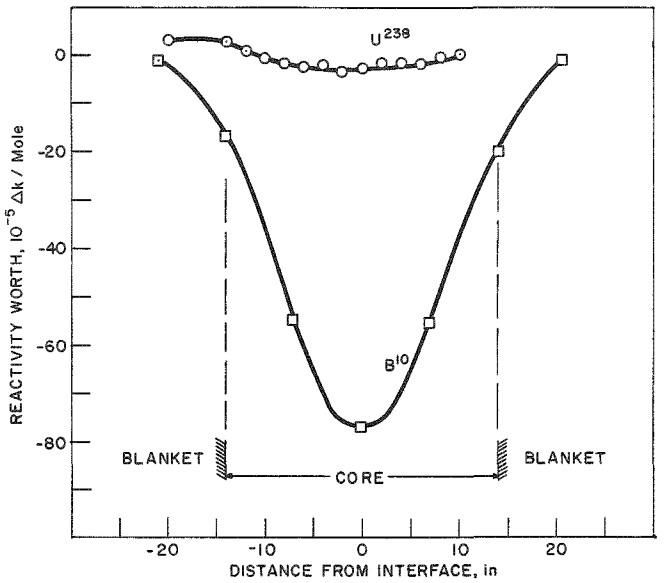

Fig. 15.

B^{10} and U^{238} Reactivity Coefficients Along Axis

It is interesting to compare the worths at the core center obtained from these traverses with those reported in previous tables. A summary of the different measurements is presented in Table XV.

Table XV

COMPARISON OF CENTRAL WORTHS FROM TRAVERSE AND SUBSTITUTION DATA

	Central Reactivity Coefficient, (Δk/mole x 10^5)		
	Central Substitutions		
Isotope	2 x 2 x 2 in.	2 x 2 x $\frac{1}{4}$ in.	Traverse ($\frac{1}{2}$ in. dia.)
U^{235}		68.4 ± 0.8	67.3 ± 3.0
U^{238}	-3.50 ± 0.1	-3.89 ± 0.7	-2.7 ± 1.0
Pu^{239}		116.5 ± 0.8	111.2 ± 2.9
B^{10}	-59.3 ± 0.4		-77.0 ± 1.0

For the fissionable materials the agreement is good, indicating that the traverse mechanism introduces no appreciable perturbation due to streaming. The results suggest that, within the accuracy of the experiments, the worth of U^{238} is independent of sample size. The difference between the B^{10} values is considered real. In the larger boron sample, the smaller reactivity effect is what would be expected due to self-shielding.

VI. SPECTRAL INDICES

Numerous experiments were performed to determine the character of the neutron flux within the reactor. Spectral indices determined from the data were compared with those derived from multigroup calculations.

A. Foil Irradiations

Foils of natural uranium and 93% enriched uranium were placed on top of fuel near the front of drawers at the center and radial edge of the core. These were irradiated during a 20-watt-hour run and then analyzed radiochemically. The number of fissions were determined by analysis for Mo^{99}, and the number of captures by analysis for Np^{239}. The results were as follows:

	Core Center	Core Radial Edge
Enriched uranium, fissions/g	$8.57 \pm 0.40 \times 10^9$	$3.65 \pm 0.33 \times 10^9$
Natural uranium, fissions/g	$3.78 \pm 0.09 \times 10^8$	$1.50 \pm 0.3 \times 10^8$
Natural uranium, captures/g	$1.04 \pm 0.02 \times 10^9$	$5.01 \pm 0.32 \times 10^8$

The cross-section ratios derived from these data are given in Tables XXII and XXIII (q.v.).

At the same time, gold foils and cans of sodium were irradiated in the central drawer, 1-P-16, at 2-in. intervals from 1 in. to 19 in. The activations were found from counting over several days. Relative activations as a function of axial position are shown in Fig. 16.

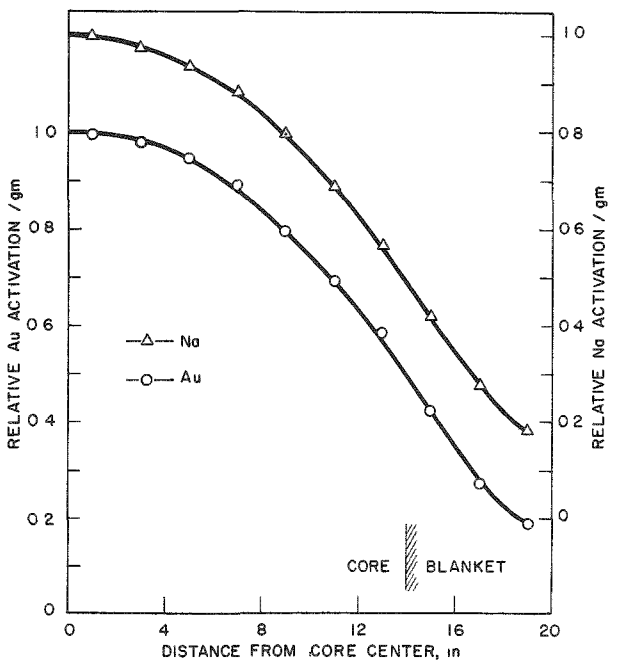

Fig. 16

Activation of Sodium and Gold along Axis

B. Fission Chamber Measurements at Core Center

Measurements of fission rates of various fissile materials at the core center were made with fission chambers of parallel-plate-type construction, because the well-defined geometry assures accurate measurements of effective cross-section ratios. The coating of fissile mass in these counters was known to within ±1%. A description of these counters has been given by Kirn,[14] and their specifications are given in Table XVI. To insure accurate results, the operating point for each counter was obtained as described by the Zeus group.[15]

Table XVI

FISSION CHAMBER SPECIFICATIONS

Counter No.	Fissile Coating	Fissile Mass (mg)	Threshold (Mev)	Isotopic Analysis, w/o							
				U^{233}	U^{234}	U^{235}	U^{236}	U^{238}	Pu^{239}	Pu^{240}	Pu^{241}
16	U^{233}	0.498		98.30	0.70			0.20			
11	U^{234}	0.496	0.3		93.44	4.87					
5	U^{235}	0.804			1.07	93.41		5.52			
24	U^{236}	0.777	0.7			3.00	96.37	0.63			
2	U^{238}	0.499	1.35			0.04		99.96			
21	Pu^{239}	0.490							99.97	0.03	
12	Pu^{240}	0.398	0.35						19.09	79.71	1.08

Chamber Dimensions - 2-in. diameter (5.08 cm)
1-in. length (2.54 cm)

The two central drawers, 1- and 2-P-16, each were modified to allow positioning of a counter at the front of the drawer. The U^{235} chamber, counter No. 5, was used as a standard and placed in 1-P-16. The other chambers were set in 2-P-16, and were thus adjacent to the reference counter at the core center during a run. For all measurements except that for Pu^{240}, fuel in the central nine drawers in each half had been unbunched (as in Figs. 12 and 13). With the reactor at constant power, counts were taken, with the counter in 2-P-16, corresponding to a standard number of counts on the U^{235} counter. The experimental results are summarized in Table XVII. Fission cross-section ratios obtained from these data are presented in the compiled Table XXII (q.v.)

Table XVII

CENTRAL FISSION CHAMBER MEASUREMENTS

Counter No.	Coating	No. of Trials	Average Count Per No. 5 Count	Experimental Standard Deviation	χ^2	Probability of χ^2
16	U^{233}	4	0.963	0.003	0.33	0.93
11	U^{234}	5	0.193	0.004	5.3	0.25
24	U^{236}	10	0.111	0.002	7.01	0.65
2	U^{238}	3	0.0233	0.0001	5.6	0.45
21	Pu^{239}	5	0.676	0.015	18.0	0.002
12	Pu^{240}	5	0.224	0.005	8.30	0.08

A statistical evaluation of the measurements is included in Table XVII and it indicates that all the results except that for Pu^{239} were statistically acceptable. Power supply instability might have been responsible for the deviations in the Pu^{239} counts.

An effort was made to determine the effects of inhomogeneity on the spectrum by observing effects on fission rates. With the central core region unbunched, an extra $\frac{1}{2}$-column of enriched U was added to each of drawers 1 and 2-P-16 (as in Fig. 13). The U^{236} fission rate was then measured. The core was returned to the normal "bunched" configuration and a count ratio again taken with the U^{236} counter. The comparative results are as follows:

Core Condition	U^{236}/U^{235} Count Ratio
Normal	0.110 ± .002
Central Region Unbunched	0.111 ± .002
Central Region Unbunched, 1 and 2-P-16 "Seeded"	0.111 ± .002

To within experimental accuracy, then, no change in fission ratios resulted from localized changes in fuel heterogeneity. Ideally, the experiment should be done with the entire core unbunched. Also, any perturbation would be better detected from the U^{238}/U^{235} ratio. However, the U^{238} counter was found to be defective at the time.

C. Axial Counter Traverses

The fission rates of U^{234}, U^{235}, U^{238}, and Pu^{239} and the $B^{10}(n,\alpha)$ reaction rate were measured along the axis of the assembly. The detectors (2 in. long and $\frac{1}{2}$ in. in diameter) were moved remotely through the same thimble used during the traverses of reactivity coefficient samples. At each axial position counts were accumulated from the traverse counters corresponding to a 10^4 count from a U^{235} fission chamber (counter No. 5) placed in 1-P-17 at the core-blanket interface. The experimental data are presented in Table XVIII. The reaction rates are plotted versus axial position in Figs. 17 through 21. Axial position was taken as the distance from the reactor center to what was judged as the center of the sensitive volume at the counter. The fissile coatings are not necessarily uniform and homogeneous, due to their method of preparation and a close observation of Figs. 17 to 21 reveals slight deviations in the estimated sensitive volume centers.

A qualitative picture of the variation of the spectra along the assembly axis can be obtained from the ratios of the count rates relative to the Pu^{239} count rates. This is possible because the Pu^{239} fission cross section varies only slightly with energy in the fast region.

Table XVIII

AXIAL TRAVERSE COUNTER DATA

Axial Position (in.)	Counts per 10^4 Counts on U^{235} Standard (Counter No. 5)				
	U^{234}	U^{235}	U^{238}	Pu^{239}	B^{10}
-30	53	1126	7		7416
-26	147	2611	10	602	12584
-22	650	9896	61	2340	40611
-18	2033	24998	265	5821	103359
-16	3558		661	9571	163386
-14	7022	62508	2080	14909	247061
-12	9930	79951	3553	19568	314063
-10	12069	94163	4455	23362	353931
-8	13927	106716	5158	26347	408142
-6	15024	116567	5817	28659	442517
-4	16312	124320	6064	30231	456018
-2	17151	127835	6251	31086	464599
-1	16994	128956	6251	31786	472504
0	16949	129722	6319	31757	486989
1	17257	129584	6433	31748	479940
2	17017	129381	6360	31614	473199
4	16277	124825	6128	30554	460802
6	15213	117952	5785	28166	440023
8	13975	107922	5230	26505	395272
10	12006	96564	4620	23232	358698
12	10364	81935	3674	20151	307669
14	7285	65697	2392	15628	244308
16	3993		578	10329	
18	2210	28592	311	6384	100090
21	1056	12500	92	3354	
Material	89.3% U^{234} 7.7% U^{235}	93.2% Enriched U	Depleted U	95% Pu^{239} 5% Pu^{240}	Enriched BF_3
Mass	3.15 mg	5.1 mg		1.96 mg	

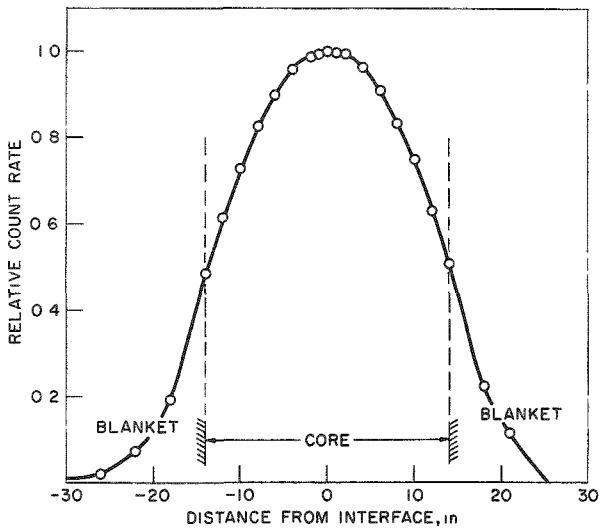

Fig. 17. U^{235} Fission Rate along Axis

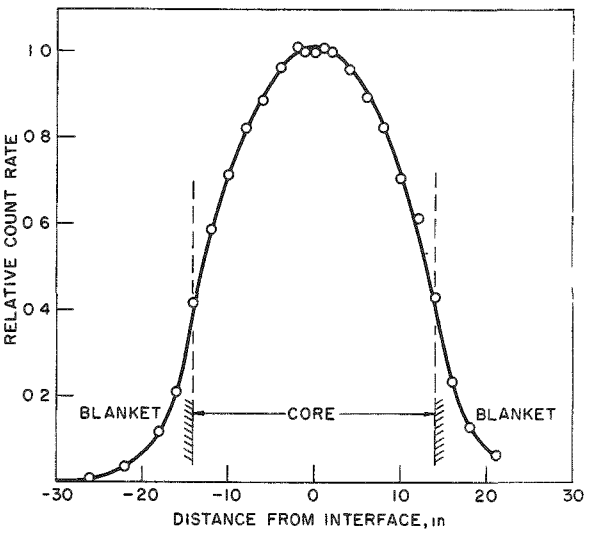

Fig. 18. U^{234} Fission Rate along Axis

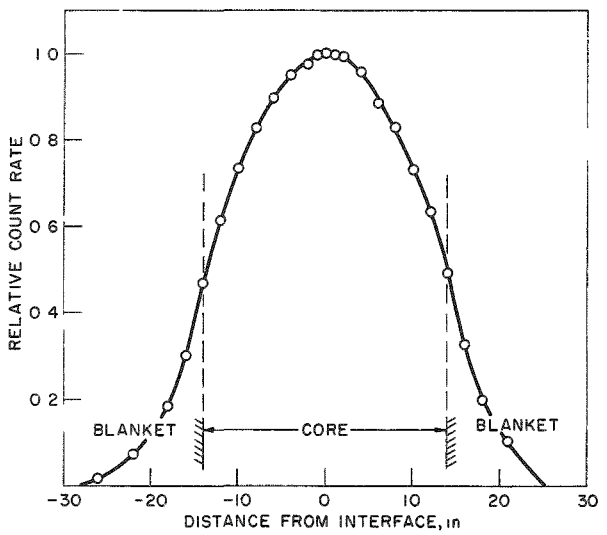

Fig. 19. Pu^{239} Fission Rate along Axis

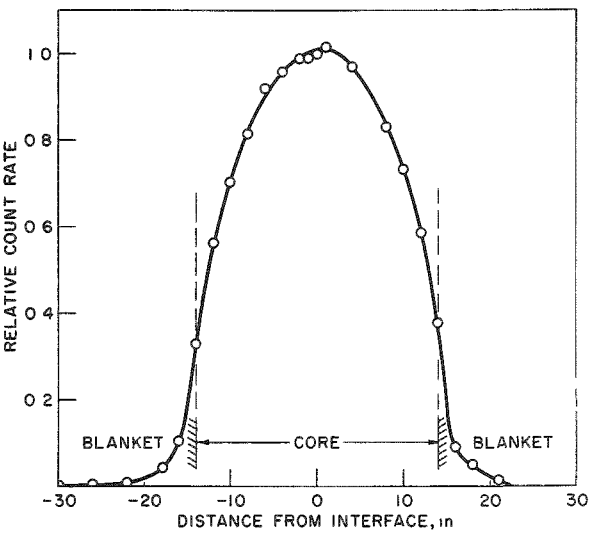

Fig. 20. U^{238} Fission Rate along Axis

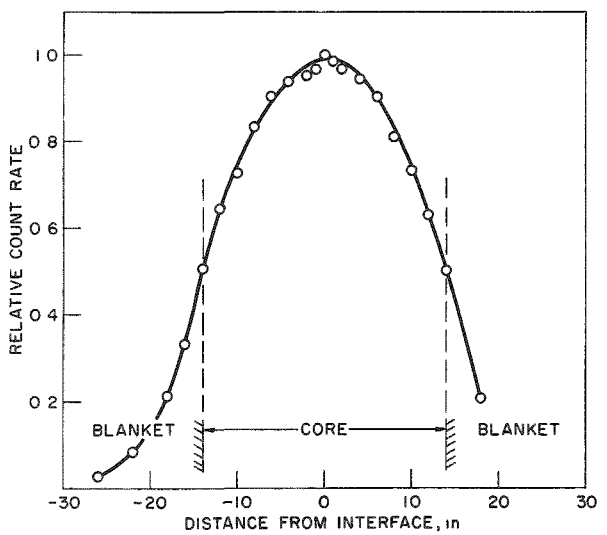

Fig. 21

B^{10} Reaction Rate along Axis.

The normalized ratios of the U^{234}, U^{235}, and U^{238} count rates relative to the Pu^{239} count rates versus axial position are shown in Figs. 22 and 23. The graphs show essentially the variation of the effective fission cross sections, but corrections for isotopic impurities have not been made. Included in Fig. 23 is a plot of the normalized ratio of the activation of gold to the Pu^{239} fission rate. Values used in obtaining the ratios in Figs. 22 and 23 were taken from the curves in Figs. 17 to 21 by taking the geometric centers of the curves as corresponding to the core center.

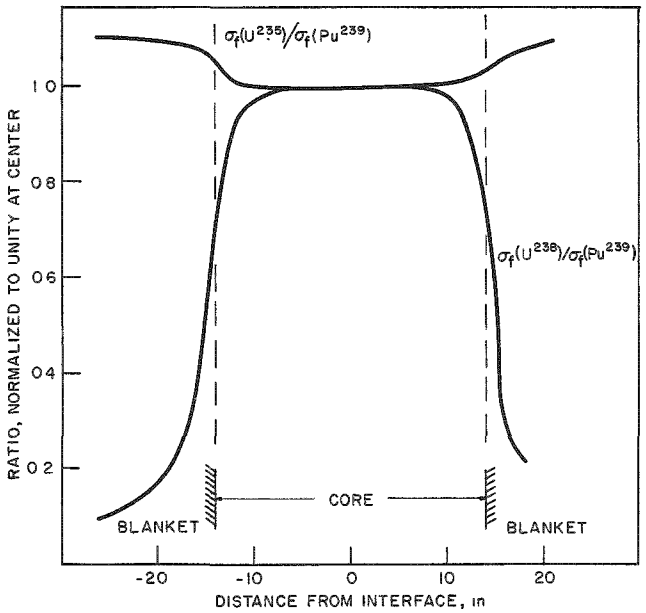

Fig. 22. Ratios of $\sigma_f(U^{235})/\sigma_f(Pu^{239})$ and $\sigma_f(U^{238})/\sigma_f(Pu^{239})$ along Axis

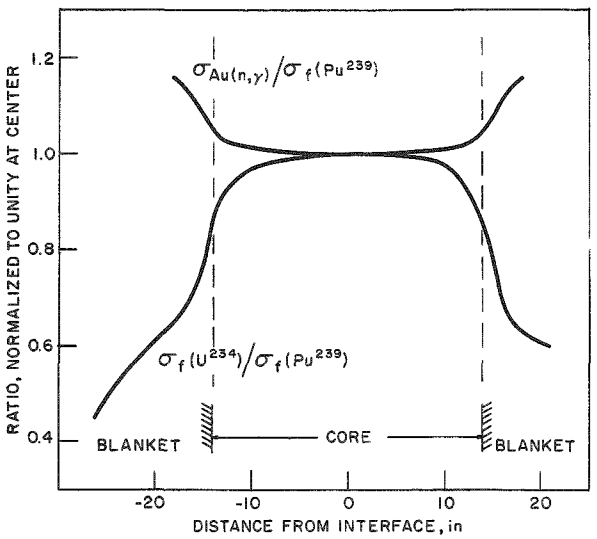

Fig. 23. Ratios of $\sigma_f(U^{234})/\sigma_f(Pu^{239})$ and $\sigma_{Au}(n,\gamma)/\sigma_f(Pu^{239})$ along Axis

D. Multigroup Spectra

The SNG calculations for k, as described in Section II, B, provide multigroup fluxes in the reactor under study at the problem mesh points. From the spectra obtained the effective fission and capture cross sections can be predicted. The problems prescribed a reflected spherical core. The group partial fluxes at the core center and core-blanket boundary obtained from two of the k calculations are given in Table XIX. The effective cross sections derived are presented in Table XXI. Multigroup fission cross-section values for U^{234} and U^{236}, which are not included in sets 58 and 135, have been constructed using BNL-325[16] as a source; these are listed in Table XX.

Table XIX

MULTIGROUP SPECTRA FROM SNG CALCULATIONS

	Core Center		Core Edge	
E_L(Mev)	16-group χ_i	11-group χ_i	16-group χ_i	11-group χ_i
3.67	0.0185		0.0145	
2.25	0.0384	0.0516	0.0280	0.0393
1.35	0.0673	0.0674	0.0478	0.0503
0.825	0.0975	0.0884	0.0782	0.0711
0.500	0.1412	0.136	0.1332	0.1326
0.300	0.137	0.117	0.1449	0.1273
0.180	0.138	0.132	0.1507	0.1388
0.110	0.108	0.107	0.1280	0.1146
0.067	0.081	0.097	0.0869	0.1083
0.041	0.081		0.0970	
0.025	0.032	0.108	0.0320	0.1213
0.015	0.039		0.0404	
0.0091	0.0135	0.067	0.0129	0.0699
0.0055	0.0046		0.0037	
0.0020	0.0026		0.0017	
0.000	0.0004	0.0276	0.0001	0.0265

Table XX

MULTIGROUP U^{234} AND U^{236} FISSION CROSS SECTIONS

	16-group			11-group		
E_L(Mev)	Group No.	$\sigma_f(U^{234})$	$\sigma_f(U^{236})$	Group No.	$\sigma_f(U^{234})$	$\sigma_f(U^{236})$
3.67	1	1.56	1.10			
2.25	2	1.53	0.87	1	1.54	0.90
1.35	3	1.45	0.74	2	1.45	0.74
0.825	4	1.20	0.43	3	1.20	0.43
0.500	5	0.90	0.06	4	0.90	0.06
0.300	6	0.24		5	0.24	
0.180	7	0.063		6	0.063	
0.110	8	0.034		7	0.034	

Table XXI

EFFECTIVE CROSS SECTIONS (IN BARNS) FROM SNG SPECTRA

	Core Center		Core-Blanket Boundary	
Cross Section	16-group (Set 135)	11-group (Set 58)	16-group (Set 135)	11-group (Set 58)
$\sigma_f(U^{233})$	2.48	2.54		
$\sigma_f(U^{234})$	0.474	0.446	0.397	0.381
$\sigma_f(U^{235})$	1.61	1.77	1.63	1.79
$\sigma_f(U^{236})$	0.153	0.143		
$\sigma_f(U^{238})$	0.065	0.061	0.048	0.046
$\sigma_f(Pu^{239})$	1.83	1.88	1.82	1.88
$\sigma_f(Pu^{240})$	0.473	0.423	0.388	0.354
$\sigma_c(U^{238})$	0.201	0.228	0.212	0.237

E. Cross-section Ratios

In Tables XXII and XXIII are compiled the calculated and experimental effective cross-section ratios derived from the various measurements and calculations. For all of the experimental values the effects of isotopic impurities have been accounted for. The ratios of the cross sections in Table XXI are used for comparison, although the validity of the multigroup spectra from which these were obtained is uncertain because of the poor determinations of k.

Table XXII

CROSS-SECTION RATIOS AT CORE CENTER

	Experimental		Theoretical: SNG Spectra		Ratio: Calc/Exp	
	Fission Chambers	U-foil Irradiations	16-group (Set 135)	11-group (Set 58)	16-group	11-group
$\sigma_f(U^{233})/\sigma_f(U^{235})$	1.470 ± 0.015		1.537	1.435	1.05	0.98
$\sigma_f(U^{234})/\sigma_f(U^{235})$	0.259 ± 0.005		0.295	0.252	1.14	0.97
$\sigma_f(U^{236})/\sigma_f(U^{235})$	0.084 ± 0.002		0.095	0.081	1.13	0.96
$\sigma_f(U^{238})/\sigma_f(U^{235})$	0.0356 ± 0.0004	0.035 ± 0.007	0.0404	0.0345	1.13	0.97
$\sigma_f(Pu^{239})/\sigma_f(U^{235})$	1.06 ± 0.02		1.139	1.062	1.08	1.00
$\sigma_f(Pu^{240})/\sigma_f(U^{235})$	0.289 ± 0.006		0.294	0.239	1.02	0.83
$\sigma_c(U^{238})/\sigma_f(U^{235})$		.115 ± 0.006	0.125	0.129	1.09	1.12
$\sigma_f(U^{233})/\sigma_f(Pu^{239})$	1.39 ± 0.03		1.353	1.351	0.97	0.97
$\sigma_f(U^{234})/\sigma_f(Pu^{239})$	0.244 ± 0.005		0.259	0.237	1.06	0.97
$\sigma_f(U^{235})/\sigma_f(Pu^{239})$	0.944 ± 0.02		0.879	0.942	.93	1.00
$\sigma_f(U^{236})/\sigma_f(Pu^{239})$	0.079 ± 0.002		0.0834	0.0758	1.06	0.96
$\sigma_f(U^{238})/\sigma_f(Pu^{239})$	0.0336 ± 0.0006	(0.033 ± 0.007)*	0.0355	0.0324	1.06	0.96
$\sigma_f(Pu^{240})/\sigma_f(Pu^{239})$	0.273 ± 0.006		0.258	0.225	0.94	0.82
$\sigma_c(U^{238})/\sigma_f(Pu^{239})$		(0.108 ± 0.006)*	0.110	0.122	1.02	1.13

*Using $\sigma_f^{29}/\sigma_f^{25} = 1.06$

Table XXIII

CROSS SECTION RATIOS AT CORE-BLANKET BOUNDARY

	Experimental		k-Calculation Spectra, Boundary of Spherical Core	
Ratio	Fission Chamber Axial Boundary	Foil Irradiation Radial Boundary	16-group (Set 135)	11-group (Set 58)
$\sigma_f(U^{234})/\sigma_f(U^{235})$	0.200 ± 0.004		0.218	0.213
$\sigma_f(U^{238})/\sigma_f(U^{235})$	0.0252 ± 0.005	0.032 ± 0.008	0.0292	0.0258
$\sigma_f(Pu^{239})/\sigma_f(U^{235})$	1.029 ± 0.020		1.119	1.049
$\sigma_c(U^{238})/\sigma_f(U^{235})$		0.130 ± 0.016	0.1305	0.1325
$\sigma_f(U^{234})/\sigma_f(Pu^{239})$	0.194 ± 0.004		0.195	0.203
$\sigma_f(U^{235})/\sigma_f(Pu^{239})$	0.972 ± 0.02		0.896	0.952
$\sigma_f(U^{238})/\sigma_f(Pu^{239})$	0.0245 ± 0.002	(0.031 ± 0.008)*	0.0261	0.0245
$\sigma_c(U^{238})/\sigma_f(Pu^{239})$		(0.126 ± 0.015)*	0.117	0.126

*Using $\sigma_f(Pu^{239})/\sigma_f(U^{235}) = 1.029$

Cross-section ratios at the core center, obtained from the absolute fission chamber measurements and the uranium foil-irradiation data, are presented in Table XXII with the multigroup values. The ratios are taken with respect to the fission cross section of U^{235} and also that of Pu^{239}. Included are the ratios of the calculated values to the experimental values.

One would expect the calculated-to-experiment ratios to lie close to one, with small random errors on each side. In the 16-group list, this is not the case. Here the high ratios with respect to U^{235} suggest that the fission cross section for U^{235} is calculated about 10% low. The ratios to the Pu^{239} fission cross section are slightly better. It would be thought that σ_f for U^{235} is known more accurately, and the ratios suggest that:

(a) The 16-group spectra does not give enough flux to the groups of lower energy; this would account for the low σ_f for U^{235} and U^{233}, and threshold-fission isotopes.

(b) The 16-group values of $\sigma_c(U^{238})$ might be generally high; since σ_c for U^{238} increases more rapidly than $\sigma_f(U^{235})$ with decreasing energy, the ratio $\sigma_c(U^{238})/\sigma_f(Pu^{239})$ should be calculated as lower than experiment, but it is not.

(c) Either the Pu^{240} or the U^{234} fission chamber measurement is in error. Both Pu^{240} and U^{234} have about the same fission threshold and asymptotic σ_f; hence their fission ratios should be nearly equal. It is possible that for one of the counters the value of the fissionable mass was inaccurate.

The ratios calculated from the 11-group spectrum are in good agreement with the measured ratios, although it is to be noted that:

(a) The capture cross section for U^{238} is calculated high by about 12%. Such an error would contribute to what has been suspected from past assemblies, viz., that Set 58 provides an underreactive U^{238}.

(b) There is a little indication that the spectrum provides slightly too few neutrons in the groups of higher energy.

Table XXIII presents experimental and calculated values for cross-section ratios at the core-blanket boundary. The experimental values are those measured in the assembly at the axial core-blanket interface and at the core radial boundary near the midplane. Compared to these are the ratios given by the spectra at the core-blanket boundary of the spherical core of the k calculations. Due to the differences in geometric situation, an intercomparison can only be approximate.

The fission ratios for the core axial edge were found from the counter data for the axial traverse, (with the aid of the count rates relative to the count rates at the core center) and the cross-section ratios obtained for the center with the absolute counters. Ratios for the core radial boundary come from the uranium foil-irradiation results; these were less accurate because of fine flux variations across the columns at the fuel drawers in which the foils were placed.

Considering the nature of the spherical model used for the k calculations, the 11-group values in Table XXIII agree quite well with experiment. The values for the 16-group set, however, exhibit the same deviations noted for the central cross-section ratios.

F. Calculated Reactivity Worths

Additional information regarding the quality of the multigroup parameters is provided by a comparison of material worths calculated by means of the group set with the measured values. The methods used to calculate the worths are (1) one-group perturbation theory; (2) multigroup perturbation theory; and (3) two-region-core k-calculations.

One-group Perturbation Theory

In recent years a perturbation theory has been developed[17-19] to determine the reactivity changes produced by introduction of small amounts of material into a reactor. This theory is of considerable importance to fast reactors, in which a perturbation causes no significant changes in the spectrum or flux shape. In the simplest form, the one-group case, the reactivity change produced by introduction of a perturbation material M in a region S of a reactor is given by[18]

$$\frac{\Delta k}{k} = \frac{\int_S [(\nu_M \sigma_{fM} + \sigma_{sM}) - g(\sigma_{fM} + \sigma_{cM} + \sigma_{sM})]\ \phi^2\ N_M dV}{\int_R \nu \Sigma_f \phi^2 dV} \quad , \quad (6.1)$$

where

$$g = 1 - \frac{1}{3\Sigma_{tr}^2} (\nabla \phi / \phi)^2$$

and N_M is the atomic density of the material. In equation 6.1, ν_M, σ_{fM}, σ_{sM}, and σ_{cM} are the microscopic cross sections (for fission neutron yield, fission, scattering, and capture) for the atoms of the perturbation material. The parameters ν, Σ_f and Σ_{tr} are the fission yield and total macroscopic fission and transport cross sections in the region of integration. The numerator is integrated over the sample volume while in the denominator the integration extends over the whole reactor.

When we are only concerned with small samples placed at the reactor center, where the flux gradient is zero, equation 6.1 reduces to

$$\frac{\Delta k}{k} = \frac{\int_S [(\nu - 1)\sigma_f - \sigma_c]_M N_M \phi^2 dV}{\int_R \nu \Sigma_f \phi^2 dV} \quad . \tag{6.2}$$

This one-group approximation does not account for reactivity effects due to spectrum changes induced by elastic and inelastic scattering. Hence its usefulness is restricted to the fissionable elements for which $(\nu - 1)\sigma_f - \sigma_c >> \sigma_s$. Using the multigroup fluxes in Table XIX, the flux-averaged values of $(\nu - 1)\sigma_f - \sigma_c$ for U^{233}, U^{235}, and Pu^{239} have been constructed, and these are presented in Table XXIV together with the measured reactivity worths.

Table XXIV

CENTRAL WORTHS AND $(\nu - 1)\sigma_f - \sigma_c$ VALUES FOR U^{233}, U^{235}, AND Pu^{239}

Material	Experimental Worth (Δk/mole x 10^5)	Flux-averaged $(\nu-1)\sigma_f-\sigma_c$ (barns)	
		11-group	16-group
U^{233}	127.2	3.688	3.648
U^{235}	68.4	2.262	2.057
Pu^{239}	116.5	3.303	3.250

The denominator of equation 6.1 is independent of the nature of the perturbation, and we can expect the values of $(\nu - 1)\sigma_f - \sigma_c$ to be proportional to the experimental worths per mole, i.e., $(\nu - 1)\sigma_f - \sigma_c = A\Delta k$. Values of A, the ratio of calculated to experimental values, are given in Table XXV.

Table XXV

RATIOS OF $(\nu-1)\sigma_f-\sigma_c$ TO THE EXPERIMENTAL WORTH

Material	11-group Values / Experimental Values	16-group Values / Experimental Values
U^{233}	2895	2866
U^{235}	3308	3006
Pu^{239}	2835	2790

The experimental measurements are considered accurate to ±2%. It is surprising to find the U^{235} values deviating as much as they do from the others.

In the case of the 16-group ratios, it appears that the $(\nu - 1)\sigma_f - \sigma_c$ value for U^{235} is over-calculated by about 6%. We have seen (Sect. VI E) that the U^{235} fission cross section derived by means of the 16-group spectrum was about 7% low. Since $\sigma_c(U^{235})$ has only minor influence, the analysis suggests that $\nu(U^{235})$ may possibly be in error by 10% on the basis of this cross-section set.

Similarly, for the 11-group set we find $(\nu - 1)\sigma_f - \sigma_c$ for U^{235} calculated apparently high by 15% and conclude that this discrepancy most likely originates in the group ν values.

The material buckling is largely dependent on the value of $(\nu - 1)\sigma_f - \sigma_c$ for the fuel material. Increasing the average fuel density of the reactor core gave a reactivity change approximately given by

$$\Delta k/k = 0.4 \Delta M/M \quad .$$

Hence, over the whole core $\Delta k/k = 0.40\, \Delta[(\nu - 1)\sigma_f - \sigma_c]$. The 11-group calculation for k gave an excess of about 6% $\Delta k/k$, which could be due mostly to the postulated +15% error in $(\nu - 1)\sigma_f - \sigma_c$ for U^{235}.

For the 16-group set, however, a value of $(\nu - 1)\sigma_f - \sigma_c$ 6% high would contribute only about 2 of the 5% excess k given by the 16-group calculation for k cited in Sect. II B. The rest of the error needs to be attributed to the parameters for the nonfissile elements in the assembly. This was investigated as far as possible by the multigroup perturbation theory analysis and the two-region core calculations.

Multigroup Perturbation Theory

According to the multigroup theory described by Glasstone and Edlund,[19] a material perturbation in a reactor yields a reactivity change of

$$\frac{\Delta k}{k} = \int\int\int_S \phi^+ \delta Q \phi dV \Big/ \int\int\int_R \phi^+ \nu \Sigma_f \phi dV \quad , \qquad (6.3)$$

where ϕ is a matrix of the group fluxes (column vector), ϕ^+ is the adjoint matrix (row vector), δQ is the perturbation matrix operator, and the product is a scalar quantity. For a region where the flux gradient is zero, the operator δQ is constructed from the material cross sections involving fission, capture, and between-group scattering.

This approach was used for fissile and nonfissile materials, using the 16-group cross-section set and the fluxes and adjoints listed in Table XXVI. For each element, the numerator of equation 6.3 was determined and then converted into an effective reactivity cross section using the value of $(\nu - 1)\sigma_f - \sigma_c$ for Pu^{239} as a normalizing factor. The results are compared in Table XXVII with the experimental cross sections derived from the measured worths, again using Pu^{239} as a reference.

Table XXVI

16-GROUP SNG CENTRAL FLUXES AND ADJOINTS

Group	Lower Energy Limit (Mev)	Partial Flux (%)	Adjoint
1	3.668	1.85	3.407
2	2.225	3.84	3.354
3	1.350	6.73	3.143
4	0.825	9.75	3.009
5	0.500	14.12	3.012
6	0.300	13.7	3.142
7	0.180	13.8	3.222
8	0.110	10.8	3.341
9	0.067	8.1	3.415
10	0.0407	8.1	3.407
11	0.025	3.2	3.486
12	0.015	3.9	3.430
13	0.0091	1.35	3.626
14	0.0051	0.46	3.694
15	0.0021	0.26	3.614
16	0.0005	0.04	3.402

Table XXVII

RESULTS OF MULTIGROUP PERTURBATION CALCULATIONS

Material	Experimental Worth (Δk/mole x 10^6)	Perturbation Theory Numerator, Eq. 6.3	Experimental σ_r (mb)	Perturbation Theory 16-group σ_r (mb)
Pu^{239}	1165	10263	3250	3250
U^{235}	684	6525	1908	2066
U^{233}	1272	11385	3548	3606
U^{238}	-35.5*	-309	-99.0	-97.9
C	10.8*	57.0	30.1	18.1
Na	9.1	31.1	25.4	9.85
Al	1.28*	8.24	3.57	2.61
Fe		-26.9		-8.52
Cr		-47.9		-15.2
Ni		-20.3		-6.43
Steel	-1.95*		5.44	-9.57**

*Average of worths in normal core and in core with "unbunched" central region.

**Using steel of composition 19 a/o Cr, 10 a/o Ni.

The multigroup perturbation analysis is seen to provide reactivity cross sections for Pu^{239}, U^{235}, and U^{233}, which are similar to those found from the one-group method. This shows the validity of the one-group treatment. It may be concluded that ν for U^{235} is given too high by Set 135.

The calculated and experimental cross sections for the light elements C, Al, Na, and Fe (SS) differ noticeably. In each case the reactivity effects of the material are underestimated. Moderation and self-shielding in the experimental samples are not considered strong enough to explain the differences. Accuracy of the calculated values depends on the factors involved, the fluxes, adjoints, cross sections for capture, and group-to-group scattering. It is suspected, and will be evidenced later, that the cross-section sets for Al and Fe are incorrect. However, with poor values given by the perturbation theory for C and Na, it appears that the fluxes and adjoints used are also in error.

Two-region Calculations

A more direct way of calculating material worths would be to recalculate k for the reactor including a perturbation region containing the material. This would account for any gross spectrum changes or self-shielding effects, if any, due to the larger sample size. A few SNG criticality calculations were performed in which the core had two regions: (a) an 8-cu-in. central region occupied by the reactivity material, (b) the remainder of the core with the normal fuel composition. For these problems, the Yiftah 16-group parameters were again used. The results are compared in Table XXVIII with experimental values computed using the experimental worths of Table XXVII and the atomic densities supplied with the 16-group set.

Table XXVIII

CENTRAL WORTHS OF 8-CU-IN. SAMPLES

Material	Experimental Worth ($\Delta k \times 10^5$)	Calculated Worth ($\Delta k \times 10^5$)
U^{238}	-37.1	-39.0
C	+19.7	+24.0
Na	+ 4.36	+ 6.0
Al	+ 1.68	+10.3
Fe	- 3.60	+10.2

Except for the values for Al and Fe, the agreement with experiment is reasonably good. Both Al and Fe are calculated highly overreactive, and this lends support to the contention that they are responsible for the extra 3% in the k-overestimate given by the 16-group set. It is possible that the calculated values are in error because of limitations of the machine code, but they are more likely due to errors in the cross-section set.

This sort of calculation depends on the material cross sections for total scattering as well as for capture and between-group scattering, but at the core center positive reactivity effects are principally related to the group-to-group scattering. That the two-region calculations overestimate worths for nonfissile materials at the core center seems to indicate that the scattering parameters are too high, giving excess transport of neutrons to energies of higher worth.

The results of the two-region calculations are generally different from the results of perturbation theory. For a comparison, the experimental and calculated cross sections are summarized in Table XXIX.

Table XXIX

EFFECTIVE REACTIVITY CROSS SECTIONS

Material	$\bar{\sigma}_r$ (mb) Experiment	$\bar{\sigma}_r$ (mb) Perturbation Theory	$\bar{\sigma}_r$ (mb) 2-region Calculation
Pu^{239}	3250*	3250*	(3250)*
U^{235}	1908	2066	
U^{233}	3548	3606	
U^{238}	-99.0	-97.9	-104
C	30.1	18.1	36.7
Na	25.4	9.85	34.9
Al	3.57	2.61	21.9
Fe		-8.52	+15.4
Steel	-5.44	-9.57	

*All values taken relative to $(\nu - 1)\sigma_f - \sigma_c$ for Pu^{239}.

It is interesting to note that the errors in the results of perturbation theory are in the opposite direction from the errors of the two-region calculations. Information regarding spectrum effect and self-shielding was also obtained from the two-region problems. The central flux and adjoint spectra from the two-region calculations were found to be almost the same as for the normal core, and only in the case of carbon is it considered that the use of the normal core spectra for the perturbation calculation may be invalid. The central flux spectrum of the Al two-region core is compared in Table XXX with that of the normal core. Also, a plot of the spatial total flux of the two-region core along with that of the normal core, (see Fig. 24) shows no central flux depression. Therefore, as mentioned before, discrepancies between experiment and perturbation theory cannot be attributed in any large degree to spectral changes or sample-size effects. Rather, it is thought that the initial fluxes and adjoints used do not represent the actual reactor.

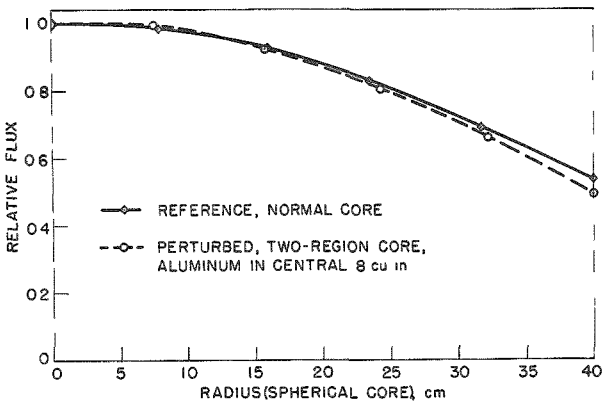

Fig. 24. Flux Shapes from SNG Calculations

If fission parameters σ_f and ν for the fuel were incorrect, this would of course give a source-term error and thus affect the flux and adjoint spectra. However, the relative group fluxes are also largely dependent on scattering. The two-region results suggest the Al- and Fe-scattering parameters are too high. At the core center, this would account for overcalculated worths of Fe and Al due to excess moderation. Over the whole reactor any excess in total scattering (essentially σ_{tr}) would decrease leakage, thereby increasing reactivity, and also alter the spectral characteristics.

G. Conclusions

We have restricted our analysis to the use of the various Argonne cross-section sets. However, the 16-group Los Alamos set[20] has been used for a reactor of this size and composition, giving a k value of 1.008. A comparison of the ANL and LASL sets shows major differences in the transport cross sections for Al and Fe in the energy range from 10 to 300 kev, i.e., the two sets $\sigma_{tr,Fe}$ and $\sigma_{tr,Al}$ differ by factors of from three to five.

Table XXX

COMPARISON OF CENTRAL SPECTRA OF Al TWO-REGION CORE AND NORMAL CORE

Group No.	ϕ_N, Normal Core (%)	ϕ_N, 2-region Core Al in Center 8 cu in. (%)
1	1.85	1.56
2	3.84	3.55
3	6.73	6.44
4	9.75	9.63
5	14.12	13.82
6	13.68	13.80
7	13.75	13.58
8	10.84	10.67
9	8.11	8.10
10	8.15	8.40
11	3.21	3.23
12	3.91	4.44
13	1.35	1.61
14	0.46	0.67
15	0.26	0.49
16	0.04	0.01

In finding the within-group-average cross sections, a flux-weighting is used at Argonne, i.e.,

$$\frac{1}{\overline{\sigma}_{tr}} = \frac{\int \phi(E) \frac{1}{\sigma_{tr}} dE}{\int \phi(E)\, dE} ,$$

where $\phi(E)$ is a representative flux within the group. On the other hand for medium Z elements the LASL group determines averages as follows:

$$\frac{1}{\overline{\sigma}_{tr}} = \frac{\int \phi(u) \frac{1}{\sigma_{tr}^2} du}{\int \phi(u) \frac{1}{\sigma_{tr}} du} ,$$

arguing that this method accounts for fine irregularities in the flux due to scattering resonances. Thus the ANL set possibly overestimated the effects of the resonances, whereas the LASL values might underestimate them slightly.

If the cross sections in the Argonne sets are modified in the LASL manner, it is believed that estimates of critical mass would be in better agreement with experimental results. At the same time, the multigroup flux and adjoint solutions of the transport equations should provide more accurate cross-section ratios and central materials worths.

We deduce, then, the need of some modifications in the Yiftah cross-section set. The ν values for U^{235} in this set, as well as for Set 58, are apparently too high in general. The values of $\sigma_f(U^{235})$ might also be off in the 16-group set. As previously stated, the transport cross sections should be re-evaluated. It would be profitable to investigate this situation further, to obtain information on the σ_{tr} of medium-Z elements by measuring central and edge reactivity worths in some future assemblies. It also appears desirable to strive for higher accuracy in reactivity measurements with the ZPR.

ACKNOWLEDGMENTS

Acknowledgments are due to G. S. Brunson for the Rossi-alpha measurements, to P. I. Amundson and R. J. Armani for assistance with the sodium and foil irradiations, to A. R. Baker for a preliminary SNG calculation, and to Mrs. N. Price and Lois Meyer for computational assistance.

REFERENCES

1. J. K. Davidson and D. Molino, The Fast Oxide Breeder-Reactor Analysis. Part II - Reactor Calculations, KAPL-1756 (1957).
2. P. Greebler, P. Aline, and J. Sueoka, Fast Oxide Breeder-Reactor Physics. Part I - Parametric Survey of 300 (e) Mw Reactor Core, GEAP-3287 (1959).
3. W. B. Loewenstein and D. Okrent, The Physics of Fast Power Reactors, A Status Report Proc. 2nd UN Int. Conf. on the Peaceful Uses of Atomic Energy, Geneva 12, 16. (1958).
4. D. Okrent, The Sensitivity of Breeding Ratio in Fast Reactors to Uncertainties in Cross Sections. Proc. of the Conf. on the Physics of Breeding, ANL-6122 (1959).
5. B. C. Cerutti et al., ZPR-III, Argonne's Fast Critical Facility, Nuclear Sci. and Engr., 1, 126 (1956).
6. G. R. Keepin, Delayed Neutrons, a Review as of October, 1955, LA-1970.
7. Reactor Physics Constants, ANL-5800, p. 418 (1958).
8. J. K. Long et al., Fast Neutron Power Reactor Studies with ZPR-III Proc. 2nd UN Int. Conf. on the Peaceful Uses of Atomic Energy, Geneva 12, 119 (1958).
9. Reactor Physics Constants, ANL-5800, p. 425 (1958).
10. H. H. Hummel et al., ZPR-V Studies, Experiment and Theory, Proc. 2nd UN Int. Conf. on the Peaceful Uses of Atomic Energy, Geneva 12, 166 (1958).
11. S. Yiftah, D. Okrent, and P. A. Moldauer, Fast Reactor Cross-Sections, Pergamon Press, New York (1960).
12. G. S. Brunson et al., Measuring the Prompt Period of a Reactor, Nucleonics, 15 (11), 32 (1957).
13. J. K. Long, op. cit., p. 130.
14. F. S. Kirn, An Absolute Fission Counter, American Nuclear Society, 2nd winter meeting (1957).
15. A. R. Baker and R. D. Smith, unpublished information.
16. Hughes and Schwartz, Neutron Cross Sections, BNL 325.
17. E. O. Pendlebury, General Perturbation Theory in Neutronics, Proc. Phys. Soc., A68, 474 (1955).
18. J. Codd, L. R. Shepherd, and J. H. Tait, Progress in Nuclear Energy - Series I, Physics and Mathematics, p. 251, McGraw Hill, New York (1956).

19. S. Glasstone and M. C. Edlund, The Elements of Nuclear Reactor Theory, Van Nostrand, New York (1952).

20. W. H. Roach, Computational Survey of Idealized Fast Breeder Reactors, Nuclear Sci. and Engr., 8, 621 (1960).

APPENDIX A

ZPR-III, Assembly 29 Specifications

ZPR Matrix Tubes	2.18 x 2.175 x 33.5-in., cross section 4.75 in.^{2}
Front Drawers	2.06 x 2.03 x 21.25-in.
Back Drawers	2.06 x 2.03 x 11.25-in.
Control Drawers	2.06 x 2.03 x 32.5-in.

Core Drawer Compositions: Core Section 1.0921 liters

Drawer Type	U^{235} (g)	U^{238} (g)	SS* (g)	Al (g)	O (g)	Total drawers
Standard	953.4	2137.0	2115.2	718.9	404.4	353
Standard Control	953.4	2137.0	1880.6	719.0	404.5	7
"Seeded"	1422.9	1644.7	2115.2	718.9	404.4	53
"Seeded" Control	1422.9	1644.7	1880.6	719.0	404.5	3

*Including matrix and SS drawer

BLANKET COMPOSITION

Region	Volume (liters)	U^{238} (kg)	U^{235} (g)	Stainless Steel (g)
14 in. to 21 in. of front drawers	0.545	8.621	17.3	385
0 to 5 in. of back drawers	0.392	6.168	12.4	285
14 to 26$\frac{1}{4}$ in. of Control drawers	0.954	13.505	27.3	826
0 to 21 in. of radial blanket drawers	1.637	25.862	51.9	1166
0 to 26 in. of coarse radial blanket	2.023	32.030	64.3	1160

DENSITIES USED TO COMPUTE VOLUME FRACTIONS

Material	Density for 100 v/o
U^{235}	18.75 g/cc
U^{238}	19.00 g/cc
SS	7.85 g/cc
Al	2.70 g/cc
O	2.55 g/cc $=.096 \times 10^{24}$ atoms/cc